Fatty Acid Synthase: A Metabolic Enzyme and Candidate Oncogene in Prostate Cancer

Toshiro Migita, Stacey Ruiz, Alessandro Fornari, Michelangelo Fiorentino, Carmen Priolo, Giorgia Zadra, Fumika Inazuka, Chiara Grisanzio, Emanuele Palescandolo, Eyoung Shin, Christopher Fiore, Wanling Xie, Andrew L. Kung, Phillip G. Febbo, Aravind Subramanian, Lorelei Mucci, Jing Ma, Sabina Signoretti, Meir Stampfer, William C. Hahn, Stephen Finn, Massimo Loda

Background Overexpression of the fatty acid synthase (*FASN*) gene has been implicated in prostate carcinogenesis. We sought to directly assess the oncogenic potential of FASN.

Methods We used immortalized human prostate epithelial cells (iPrECs), androgen receptor–overexpressing iPrECs (AR-iPrEC), and human prostate adenocarcinoma LNCaP cells that stably overexpressed FASN for cell proliferation assays, soft agar assays, and tests of tumor formation in immunodeficient mice. Transgenic mice expressing FASN in the prostate were generated to assess the effects of FASN on prostate histology. Apoptosis was evaluated by Hoechst 33342 staining and by fluorescence-activated cell sorting in iPrEC-FASN cells treated with stimulators of the intrinsic and extrinsic pathways of apoptosis (ie, camptothecin and anti-Fas antibody, respectively) or with a small interfering RNA (siRNA) targeting *FASN*. FASN expression was compared with the apoptotic index assessed by the terminal deoxynucleotidyltransferase-mediated UTP end-labeling method in 745 human prostate cancer samples by using the least squares means procedure. All statistical tests were two-sided.

Results Forced expression of FASN in iPrECs, AR-iPrECs, and LNCaP cells increased cell proliferation and soft agar growth. iPrECs that expressed both FASN and androgen receptor (AR) formed invasive adenocarcinomas in immunodeficient mice (12 of 14 mice injected formed tumors vs 0 of 14 mice injected with AR-iPrEC expressing empty vector ($P < .001$, Fisher exact test); however, iPrECs that expressed only FASN did not. Transgenic expression of FASN in mice resulted in prostate intraepithelial neoplasia, the incidence of which increased from 10% in 8- to 16-week-old mice to 44% in mice aged 7 months or more ($P = .0028$, Fisher exact test), but not in invasive tumors. In LNCaP cells, siRNA-mediated silencing of FASN resulted in apoptosis. FASN overexpression protected iPrECs from apoptosis induced by camptothecin but did not protect iPrECs from Fas receptor–induced apoptosis. In human prostate cancer specimens, FASN expression was inversely associated with the apoptotic rate (mean percentage of apoptotic cells, lowest vs highest quartile of FASN expression: 2.76 vs 1.34, difference = 1.41, 95% confidence interval = 0.45 to 2.39, $P_{trend} = .0046$).

Conclusions These observations suggest that *FASN* can act as a prostate cancer oncogene in the presence of AR and that FASN exerts its oncogenic effect by inhibiting the intrinsic pathway of apoptosis.

J Natl Cancer Inst 2009;101:519–532

Fatty acid synthase (FASN) is a key enzyme for the synthesis of long-chain fatty acids from acetyl-coenzyme A (CoA) and malonyl-CoA that uses reduced nicotinamide adenine dinucleotide phosphate as a cofactor. Fatty acid synthesis occurs at very high rates in tumor tissues, as was first demonstrated more than half a century ago in a [^{14}C]glucose incorporation study that showed that almost all fatty acids in rodent tumor cells derive from de novo synthesis even in rodents that had an adequate nutritional supply (1). FASN is minimally expressed in most normal human tissues except the liver and adipose tissue, where it is expressed at high levels (2). FASN expression is markedly increased in several human cancers compared with the corresponding normal tissue, and its overexpression in tumors has been associated with a poor prognosis (3–12).

Affiliations of authors: Department of Medical Oncology, Dana-Farber Cancer Institute, Harvard Medical School, Boston, MA (TM, AF, MF, CP, GZ, FI, EP, ES, CF, WX, CG, SS, ML, WCH); Department of Pathology, Brigham and Women's Hospital, Boston, MA (CG, SS, SF, ML); the Center for Molecular Oncologic Pathology, Dana-Farber Cancer Institute, Harvard Medical School, Boston, MA (SF, ML); Channing Laboratory, Brigham and Women's Hospital, Boston, MA (LM, JM, MS); Department of Epidemiology, Harvard School of Public Health, Boston, MA (LM, JM, MS); Department of Pediatric Oncology, Children's Hospital, Boston, MA (ALK); Duke Institute for Genome Science, Durham, NC (PGF); The Broad Institute of Harvard and MIT, Boston, MA (ML, WCH, AS).

Address correspondence to: Massimo Loda, MD, Dana-Farber Cancer Institute, D1536, 44 Binney Street, Boston, MA 02115 (e-mail: massimo_loda@dfci.harvard.edu).

See "Funding" and "Notes" following "References."

DOI: 10.1093/jnci/djp030

CONTEXT AND CAVEATS

Prior knowledge

Fatty acid synthase (FASN)—a key enzyme in the synthesis of long-chain fatty acids—is overexpressed in prostate intraepithelial neoplasia compared with adjacent normal tissue and in metastatic prostate cancer. Several studies have shown that inhibition of *FASN* gene expression in various cancer cell lines via RNA interference–mediated silencing or chemical inhibitors induces apoptosis, suggesting that FASN overexpression may protect prostate epithelial cells from apoptosis.

Study design

A molecular examination of the effects of *FASN* expression in human prostate cancer cell lines, human prostate cancer samples, and mouse xenograft models.

Contribution

FASN can act as a prostate cancer oncogene in mouse models, and FASN exerts its oncogenic effect by inhibiting the intrinsic pathway of apoptosis.

Implications

Drug that target FASN may be an effective treatment for prostate cancer.

Limitations

Only one of many potential mechanisms of FASN-mediated oncogenicity—inhibition of apoptosis—was studied. The models used did not address the role played by lipid-modifying enzymes on FASN enzymatic products, specifically palmitate. Overexpression of *FASN* as a transgene did not result in invasive adenocarcinomas in the mouse model.

From the Editors

FASN protein function and expression has been extensively analyzed in human tumors (3–6). We previously showed that FASN is overexpressed in prostate intraepithelial neoplasia (PIN) compared with adjacent normal tissue, suggesting that it plays a role in the initial phases of prostate tumorigenesis, and in metastatic prostate cancer, suggesting that it may function as a mediator of biological aggressiveness (7). Importantly, Rossi et al. (7) demonstrated that FASN-overexpressing prostate cancers display a characteristic gene expression signature, and Shah et al. (13) found that one-fourth of human prostate cancers analyzed by fluorescent in situ hybridization have genomic amplification of *FASN*. From a functional standpoint, pharmacological approaches to decrease expression of FASN have been shown to result in growth inhibition of various tumor cell lines including those derived from prostate cancer and/or prostate cancer tumor xenografts in vivo (14–16).

Human prostate cancer is a common and clinically heterogeneous disease that comprises biologically distinct subtypes. Genome-wide analyses and epidemiological studies have identified only a small number of candidate genes that may be associated with either hereditary or sporadic prostate cancer (17–19). By contrast, emerging evidence suggests that high-fat diets and obesity are risk factors for prostate cancer (20–29). Indeed, a lipogenic phenotype is a distinctive feature of many cancer cell types including prostate cancer cells (10).

The lipogenic phenotype that results from alterations in fatty acid metabolism suggests that FASN protein overexpression may play an important role in prostate cancer initiation and maintenance. However, it remains unclear how prostate tumor cells acquire a selective growth advantage through FASN protein overexpression and how deregulated lipid metabolism contributes to transformation or tumor progression. Several studies have shown that inhibition of *FASN* gene expression in various cancer cell lines via RNA interference–mediated silencing or chemical inhibitors induces apoptosis (14–16,30). In addition, it has been reported that FASN inhibitor–mediated cytotoxicity can be reversed with palmitate, the final product of FASN catalytic activity (15,31). These observations suggest that FASN overexpression may protect prostate epithelial cells from apoptosis.

Based on the evidence that FASN is overexpressed in prostate cancer and that it may protect tumor cells from apoptosis, we proposed, and subsequently set out to demonstrate, that *FASN* is a bona fide oncogene (32). We overexpressed *FASN* in immortalized, nontransformed human prostate epithelial cells and in transgenic mice and assessed the consequences of overexpression on prostate cell transformation.

Materials and Methods

Cell Lines and Culture Conditions

Immortalized human prostate epithelial cells (iPrECs) and androgen receptor–overexpressing iPrECs (AR-iPrECs) were engineered as previously described (33). Briefly, human prostate primary epithelial cells (PrECs) were obtained from BioWhittaker (Rockland, Maine) and propagated in defined medium (PrEGM) (Cambrex, East Rutherford, NJ) as recommended. iPrECs were infected with amphotropic retroviruses encoding the SV40-large T antigen and small T antigen and *hTERT*. Wild-type androgen receptor (AR) was introduced using an AR complementary DNA (cDNA) cloned into a pWZL retrovirus containing a blasticidin selection cassette (Invitrogen, Carlsbad, CA).

Human prostate adenocarcinoma LNCaP cells were obtained from American Type Culture Collection (ATCC, Manassas, VA). The 7536–base pair human FASN cDNA previously generated by ligation of four fragments (16) and fused to internal ribosomal entry site (IRES) and luciferase (Luc) sequences was subcloned in the pBabe retroviral vector (Addgene, Cambridge, MA), resulting in the mammalian retroviral expression construct pBabe-FASN-IRES-Luc, as confirmed by DNA sequencing. This construct was used to obtain stable FASN-expressing cell lines. Human embryo kidney 293T cells (from ATCC) were cotransfected with pBabe-FASN-IRES-Luc or pBabe empty vector (EV) as control and the packaging plasmid pCL (Imgenex, San Diego, CA) using Fugene6 transfection reagent (Roche, Indianapolis, IN) according to the manufacturer's instructions. The retrovirus containing supernatant of the transfected 293T cells was used to infect iPrECs, AR-iPrECs, and LNCaP cells, as previously described (16), to generate iPrEC-FASN, AR-iPrEC-FASN, FASNCaP cells, respectively, and the corresponding control cells (iPrEC-EV, AR-iPrEC-EV, and LNCaP-EV, respectively). Infected cells were selected by their ability to grow in medium containing 2 μg/mL

puromycin (Sigma, St Louis, MO). iPrECs, AR-iPrECs, their derivatives, and iPrEC-H-ras^{Val12} cells [iPrECs which express the glycine 12 → valine mutated version of the *HA-RAS* gene; generated by Berger et al. (33)] were grown in P_2EGM medium (Cambrex). LNCaP cells and their derivatives were grown in RPMI-1640 medium (Invitrogen) containing 10% fetal bovine serum (Sigma) and 1% penicillin–streptomycin (Invitrogen).

5-Bromodeoxyuridine Incorporation Assay

iPrEC-EV, iPrEC-FASN, AR-iPrEC-EV, and AR-iPrEC-FASN cells were cultured for 2 days in six-well plates (3×10^5 cells per well) and 10 μM 5-bromodeoxyuridine (BrdU) (Upstate, Charlottesville, VA) was added to the culture medium 1 hour before harvesting. The cells were fixed in ice-cold 70% ethanol, denatured in 2 mol/L HCl, followed by neutralization with 0.1 M sodium borate, and finally stained with fluorescein isothiocyanate (FITC)-conjugated anti-BrdU monoclonal antibody (BD Biosciences, San Jose, CA), according to the manufacturer's instructions. Propidium iodide (PI) was used as the nuclear counterstain. The cells were analyzed by flow cytometry (10 000 cells per sample) to determine the percentage of cells that had incorporated BrdU.

Anchorage-Independent Growth Assay

iPrEC-EV, iPrEC-FASN, or iPrEC-H-ras^{Val12} cells were mixed with 0.4% top agar and layered over 0.6% bottom agar, in triplicate, in six-well plates (5×10^3 cells per well) (BD Biosciences, Franklin Lakes, NJ). The cells were allowed to grow for 3 weeks, at which time colonies larger than 200 μm were counted with the use of the publicly available Image J software (version 1.41; http://rsbweb.nih.gov/ij/index.html). AR-iPrEC-EV, AR-iPrEC-FASN, LNCaP-EV, and FASNCaP cells were assessed in the same manner.

In Vivo Studies

All experiments involving mice were conducted according to animal-use protocols that were approved by the Institutional Animal Care and Use Committee of the Dana-Farber Cancer Institute.

Generation of Transgenic Mice With Prostate-Specific Expression of FASN. We created a construct for prostate-specific expression of *FASN* in mice that included the androgen-responsive probasin promoter (ARR2-PB), the full-length human FASN cDNA, an internal ribosome entry site, the luciferase reporter gene, and a polyadenylation signal sequence. Injection of this construct into the pronuclei of fertilized mouse eggs (derived from an Friend leukemiavirus B strain background) was performed by the transgenic mouse core facility at Dana-Farber Cancer Institute. Transgenic founder mice were generated according to standard procedures. Identification of founder mice was confirmed by in vivo bioluminescence imaging after intraperitoneal injection of mice with D-luciferin (75 mg per kg body weight; Promega, Fitchburg, WI) followed by whole animal imaging with the use of a Xenogen IVIS 100 imaging system (Caliper Life Science, Hopkinton, MA). Both wild-type and FASN-transgenic mice were killed by CO_2 asphyxiation 30 minutes after injection with luciferin. The three lobes of the prostate, the bladder, the preputial gland, the kidneys, and the liver were then excised and placed in phosphate-buffered saline (PBS) in 24-well plates for immediate imaging as described above.

Transgenic mice were genotyped by polymerase chain reaction (PCR) using three pairs of primers: forward 5′-TGCACC-TTGTCAGTGAGGTC-3′ and reverse 5′-CGGAGTGAA-TCTGGGTTGAT-3′ located in the 3′ region of the rat probasin promoter and in the 5′ region of the *FASN* transgene, generating a 376-bp amplicon; forward 5′-CCAGGGATTTCAGTCGATGT-3′ and reverse 5′-AATCTCACGCAGGCAGTTCT-3′ located in the luciferase gene, generating a 185-bp amplicon; and forward 5′-CTAA-CGTTACTGGCCGAAGC-3′ and reverse 5′-AGGAACTGCTT-CCTTCACGA-3′ located in the IRES sequence, generating a 202-bp amplicon. Histological slides of ventral, anterior, and dorsolateral lobes of the prostates from male transgenic mice at 8–16 weeks of age (28 mice), at 4–7 months of age (59 mice), and at 7 months to 1 year of age (29 mice) were evaluated for the presence or absence of hyperplasia as well as for PIN and compared in a blinded fashion with 40 age-matched, nontransgenic control littermates by two pathologists with extensive experience in murine pathology (M. Loda and S. Signoretti). In vitro luciferase assay, PCR-based genotyping, or immunoblot analyses were performed on extracts from the hemilobe of the prostate that was not used for histopathology.

Xenografts. A 1:1 (vol:vol) mixture of 5×10^6 LNCaP-EV or FASNCaP cells and Matrigel in a total volume of 200 μL was injected subcutaneously into the right flank of 6-week-old male athymic nu/nu immunodeficient mice (purchased from Charles River Laboratories, Wilmington, MA; n = 9 mice per group). AR-iPrEC-EV or AR-iPrEC-FASN cells were also injected as described above (5×10^6 cells per mouse; 15 mice per group). Tumor size was monitored by caliper measurements every 3 days, and the mice were killed by CO_2 asphyxiation when the tumor size reached a diameter of approximately 1.5 cm. Either 5×10^6 AR-iPrEC-EV or AR-iPrEC-FASN cells, in a 1:1 mixture of P_2EGM medium and Matrigel, were injected into the anterior lobes of the prostates of 21 mice (8 for AR-iPrEC-EV and 13 for AR-iPrEC-FASN cells) in a total volume of 20 μL as previously described (33). Mice were killed by CO_2 asphyxiation 6 weeks after injection of the cells; the anterior lobes of the prostate of each mouse were resected, fixed in formalin, embedded in paraffin, and stained with hematoxylin–eosin (H&E).

Immunoblot Analysis

iPrEC-EV, iPrEC-FASN, AR-iPrEC-EV, AR-iPrEC-FASN, LNCaP-EV, and FASNCaP cells, as well as freshly frozen mouse prostate lobe tissues were lysed in 1% 3[(3-cholamidopropyl) dimethylammonio]-propanesulfonic acid buffer (Boston BioProducts, Worcester, MA), and the resulting cell extracts were cleared by centrifugation at 16 000*g*. Equal amounts of proteins from the supernatants, as measured by the Bradford method, were boiled in 2× Laemmli buffer, a reducing and denaturating loading buffer containing 4% sodium dodecyl sulfate (SDS), 20% glycerol, 10% beta-2-mercaptoethanol, 0.004% bromphenol blue, and 0.125 M Tris–HCl (pH 6.8), resolved by electrophoresis on 4%–12% polyacrylamide gels (Invitrogen), and transferred to polyvinylidene difluoride membranes (Millipore, Billerica, MA). The membranes were probed with the following antibodies:

mouse monoclonal anti-FASN (1:10 000 dilution; BD Biosciences), rabbit polyclonal anti–poly (ADP-ribose) polymerase (PARP, 1:1000 dilution; Cell Signaling, Danvers, MA), and mouse monoclonal anti–β-actin (1:10 000 dilution; Sigma). Immunocomplexes were detected with the use of horseradish peroxidase–conjugated secondary antibodies (Bio-Rad, Hercules, CA) and enhanced chemiluminescence (PerkinElmer, Waltham, MA).

Histopathology and Immunohistochemistry

Prostates were removed from transgenic mice, mice that received the orthotopic implants, and control mice. Prostates were microdissected to isolate the dorsolateral, ventral, and anterior lobes; seminal vesicles were isolated as well. Dissected tissue samples were fixed overnight in 10% formalin, processed in a VIP 2000 histological processing instrument (Sakura, Torrance, CA), and embedded in paraffin. Sections of formalin-fixed paraffin-embedded (FFPE) tissues (5 μm thick) were stained with H&E. The largest diameter of each lobe was assessed on the slide, and the number of acini present in the largest diameter section of each lobe was counted. Immunohistochemistry was performed by use of an automated i600 immunostainer (Biogenex, San Ramon, CA) on serial 5-μm sections from mouse tissue blocks and on human tissue microarray (TMA) sections by use of a standard avidin–biotin–peroxidase method that included 3,3′-diaminobenzidine as the peroxidase substrate and the following primary antibodies: rabbit polyclonal antibody to FASN (1:200 dilution; Assay Designs, Ann Harbor, MI); rabbit monoclonal antibody to Ki67 (1:100 dilution; Vector Laboratories, Burlingame, CA); mouse monoclonal antibody to SV40-large T antigen (1:50 dilution; Santa Cruz, Santa Cruz, CA); and rabbit polyclonal antibody to AR (1:100 dilution; Upstate, Billerica, MA). Each staining required antigen retrieval in citrate–PBS buffer (pH 6.0). Apoptosis in mouse and human FFPE tissue sections was studied using the Apoptag peroxidase in situ assay (Chemicon International, Billerica, MA) according to the manufacturer's instructions. The apoptotic rate was independently evaluated by two pathologists (Alessandro Fornari and Michelangelo Fiorentino) as the number of stained apoptotic cells divided by the total number of prostate epithelial cells. At least 200 cells per two high-power microscopic fields were counted per core and three cores per patient were present on the TMA. FASN expression was rated semiquantitatively based on antibody staining intensity on a scale of 0–3, where 0 represented the FASN staining intensity equal to that in prostate epithelial cells from wild-type mice and 3 represented the maximum staining intensity.

We also examined the correlation between FASN immunohistochemical expression and apoptosis assessed using the Apoptag assay in archival prostatectomy specimens from 745 men with prostate cancer that were included on nine high-density TMAs described above. These TMAs also included representative normal prostate tissue cores as controls. The men were participants in the Health Professionals Follow-up Study (http://www.hsph.harvard.edu/hpfs/) and the Physicians' Health Study (http://phs.bwh.harvard.edu/) and were diagnosed with prostate cancer between 1982 and 2004 (34–36). The median age (SD) at cancer diagnosis was 66 years (3.7 years); 61% of the men had a Gleason score of 7, and 15% had a Gleason score of 8 or higher. All experiments involving human specimens were approved by the institutional review board (authorization number BWH 2001-P-000228, "Nutritional and Biochemical/Genetic Markers of Cancer").

RNA Interference

LNCaP cells were transiently transfected with a small interfering RNA (siRNA) that silences expression of *FASN* as previously described (14). The sequence of the FASN-targeted siRNA (5′-TGGAGCGTATCTGTGAGAA-3′) was chosen out of five sequences available because it was most efficient at reducing FASN mRNA and protein levels. We therefore used this siRNA for all the experiments. As a nonspecific siRNA control, we used a scrambled-sequence siRNA duplex (5′-GCGCGCTTTGTAGGATTCG-3′); both siRNAs were synthesized by Dharmacon (Lafayette, CO). LNCaP cells were transiently transfected with 20 nM siRNA-targeting FASN or scrambled siRNA in 60-mm dishes (5×10^5 cells per dish) with the use of Lipofectamine RNAiMAX reagent (Invitrogen) according to the manufacturer's instructions and were used for apoptosis assays and measurements of intracellular levels of reactive oxygen species (ROS) measurements at 24, 48, 72, 96, and 120 hours after transfection.

Apoptosis Assays

iPrEC-EV, iPrEC-FASN, LNCaP, and FASNCaP cells were seeded in 60-mm dishes (1×10^6 cells per dish) and treated for up to 20 hours with camptothecin (0–100 nM; Calbiochem, Gibbstown, NJ) or a monoclonal anti-Fas antibody (0–500 ng/mL, clone CH-11; MBL International, Woburn, MA). Cells treated with Fas were costimulated with cycloheximide (50 μg/mL; Calbiochem) to increase their susceptibility to apoptosis (37). Cells were incubated in a 10-μg/mL solution of Hoechst 33342 for 30 minutes and apoptotic cells were counted. The apoptotic rate was measured as the percentage of apoptotic cells by Hoechst 33342 staining. Similar results were obtained by flow cytometry (data not shown).

Changes in the mitochondrial membrane potential were also assessed as an indirect measure of apoptosis among iPrEC-EV and iPrEC-FASN cells treated with campthotecin. Following 18 hours of exposure to the drug, 2×10^6 cells were harvested and incubated in suspension with the cationic fluorescent dye rhodamine 123 (100 nM concentration in P_2EGM medium) at 37°C for 30 minutes, then washed with PBS and resuspended in PI (1 μg/mL in PBS). Rhodamine 123 incorporation was assessed by flow cytometry analysis. Changes in the mitochondrial membrane potential were calculated by subtracting the number of PI-negative and rhodamine 123–positive cells after treatment from the number before treatment.

LNCaP cells were plated in 60-mm dishes (5×10^5 cells per dish) and treated with anti-FASN siRNA (for up to 120 hours) as described above. To rescue apoptosis, 100 μM palmitatein in 0.1% bovine serum albumin (BSA) was added to the cells from a stock solution of 10 mM palmitate in 10% BSA in water (both from Sigma). Apoptosis was measured by immunoblot analysis of whole-cell lysates using an antibody specific for PARP (1:1000 dilution; Cell Signaling) and flow cytometry. LNCaP cells were used for both fluorescence-activated cell sorting and immunoblotting simultaneously, pelleted, washed with PBS, and fixed with ice-cold 80% ethanol. The cells were resuspended in PBS and PI was added to a final concentration of 50 mg/mL, and the samples were subjected to flow cytometry. Flow cytometric analysis was carried out

using FACSCalibur (BD Biosciences) and cells with sub-G1 DNA content (ie, apoptotic cells) were quantified with CellQuest (BD Biosciences) and ModFit LT3.0 software (Verity Software House, Topsham, ME). Cells with sub-G1 DNA content were quantified.

Measurement of ROS

LNCaP cells (2×10^6 cells per assay) were treated with FASN siRNA for 24, 48, and 72 hours, or FASN siRNA and palmitate for 72 hours as described above. The scrambled-sequence siRNA served as a control for the experiment. Following treatment, the cells were washed once with PBS and incubated with 10 μM carboxy-H_2DCFDA, a fluorescent indicator of intracellular levels of ROS (Molecular Probe, Carlsbad, CA), for 30 minutes at 37°C in PBS. The cells were harvested and analyzed by flow cytometry using CellQuest software.

Castration-Induced Apoptosis in the Prostate Gland of Transgenic Mice

Male mice (12 wild-type mice and 12 *FASN*-transgenic mice) were castrated under anesthesia. On day 0 (ie, just before castration) and on days 3 and 7 after castration, we removed the prostate gland from four mice of each genotype per time point. The prostate glands were dissected, fixed in 10% formalin overnight, processed through a graded alcohol series and xylene, and embedded in paraffin. Paraffin sections (5 μm thick) were cut and mounted on glass slides. The sections were dewaxed, and then stained with H&E or used for immunohistochemical staining for FASN or for apoptotic cell detection with Apoptag as described above.

Statistical Analysis

Data were summarized as the number (and percentage) of samples or as mean or median values (with 95% confidence intervals [CIs]). Differences between groups were evaluated with the Student *t* test for continuous values and with the Fisher exact test for categorical variables. Comparisons between tissues from transgenic and implanted mice and paired control mice were conducted using the Wilcoxon signed rank test. The relationships between continuous variables were assessed using the Spearman correlation coefficient. In the analysis of human samples, we categorized case patients by quartiles of FASN expression based on the distribution among all patients and compared the percentage of apoptosis using the least squares means procedure (38) and conducted tests of trend using linear regression, controlling for age and body mass index at diagnosis. Statistical analysis was undertaken using SAS version 9 (SAS Institute, Cary, NC); all statistical tests were two-sided, and *P* less than .05 was considered statistically significant.

Results

Effect of *FASN* Overexpression on Immortalized Prostate Epithelial Cells

As a first step toward assessing the oncogenic properties of FASN, we overexpressed this enzyme in nontransformed prostate epithelial cells. We previously reported that immortalized nontransformed prostate epithelial cells (iPrECs) that were stably transfected with an expression vector containing the validated oncogenes Myc or H-ras^{Val12} or the activated catalytic subunit of the phosphatidylinositol 3-kinase p110 α formed tumors when injected into nude mice (33). To compare the oncogenic potential of *FASN* with that of the oncogenes mentioned above, we generated immortalized iPrECs that were stably transfected with an expression vector encoding FASN (iPrEC-FASN) or with empty vector (iPrEC-EV). We initially compared cell proliferation in these isogenic clones by use of the BrdU incorporation assay. We found that FASN overexpression conferred a statistically significant proliferative advantage to iPrECs in terms of the percentage of BrdU incorporating cells (iPrEC, FASN vs empty vector: 24.81% vs 22.66%, difference = 2.15%, 95% CI = 1.55% to 2.75%; $P = .0042$). Given that *FASN* is an androgen-regulated gene (33), we next generated iPrEC-FASN and iPrEC-EV cells that stably express the AR (AR-iPrEC-FASN and AR-iPrEC-EV, respectively). Similar results were obtained with these cells (percentage of AR-iPrECs incorporating BrdU, FASN vs empty vector: 30.18% vs 22.82%, difference = 7.36%, 95% CI = 5.4% to 9.3%; $P = .0037$) (Figure 1, A). We confirmed that FASN expression was considerably higher in iPrECs, AR-iPrECs, and LNCaP cells that were stably transfected with the FASN expression construct than in the isogenic control cells stably transfected with the empty vector (Figure 1, B). In the anchorage-independent growth assay, iPrEC-FASN cells formed statistically significantly more colonies in soft agar than iPrEC-EV cells (325.4 vs 42.2 colonies, difference = 283.2 colonies, 95% CI = 233.2 to 333.2 colonies; $P < .001$). The number of foci formed by iPrEC-FASN cells was intermediate between the numbers formed by iPrEC-EV cells and by iPrEC-H-ras^{Val12} cells (42.2 and 897.19 foci, respectively). AR-iPrEC-FASN cells also formed a statistically significantly greater number of colonies than AR-iPrEC-EV cells (577 vs 107.3, difference = 469.7, 95% CI = 395.7 to 543.6; $P < .001$) (Figure 1, C). We next examined whether the overexpression of FASN in transformed prostate LNCaP cells would affect their ability to form colonies in soft agar. LNCaP cells that stably overexpressed FASN (FASNCaP cells) formed a statistically significantly greater number of colonies in soft agar compared with vector-transfected LNCaP cells (833.7 vs 240.2, difference = 593.4, 95% CI = 550.6 to 636.2; $P < .001$) (Figure 1, C).

We next examined the ability of immortalized prostate epithelial cells stably transfected with FASN to form tumors in vivo. iPrEC-H-ras^{Val12} cells formed palpable tumors within 3 weeks after subcutaneous injection into immunodeficient mice (five of six injected mice formed tumors), whereas iPrEC-FASN cells did not, regardless of whether the iPrEC-FASN cells were injected subcutaneously (none of 10 injected mice formed tumors) or orthotopically (two of 10 injected mice formed tumors). Importantly, AR-iPrEC-FASN cells formed invasive adenocarcinomas when injected either subcutaneously (12 of 14 mice injected formed tumors vs 0 of 14 mice injected with AR-iPrEC-EV) or orthotopically (nine of 13 mice injected formed tumors vs two of eight mice injected with AR-iPrEC-EV into immunodeficient mice; $P < .001$ for both comparisons, Fisher exact test). As expected, the tumorigenic AR-iPrEC-FASN cells in murine prostate tumors expressed FASN, SV40-large T antigen, and AR (Figure 1, D). We also examined tumor formation when LNCaP cells transfected with empty vector or *FASN* were injected subcutaneously in immunodeficient mice. Stable expression of *FASN* in LNCaP cells allowed

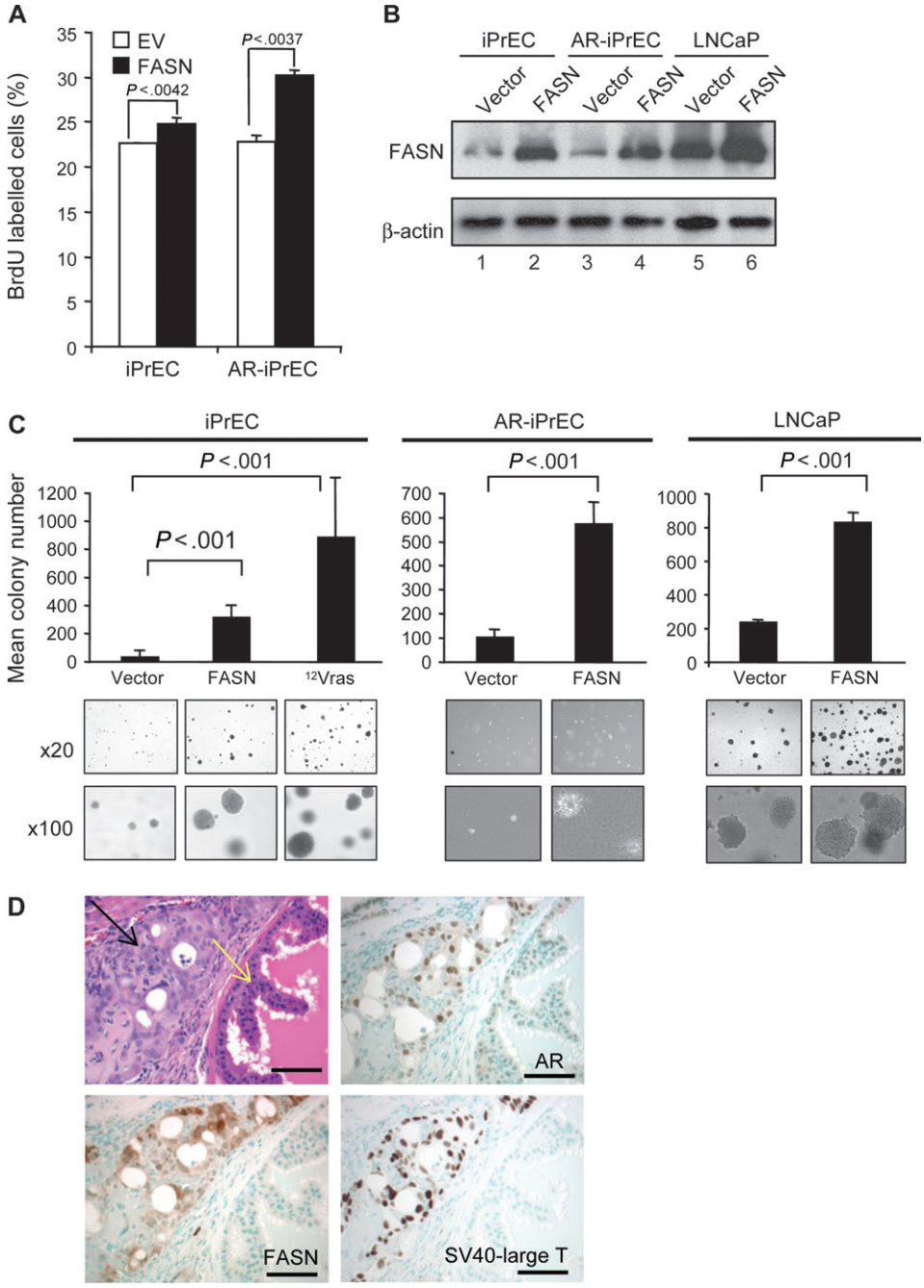

Figure 1. Effect of fatty acid synthase (FASN) overexpression on cell proliferation, growth in soft agar, and tumorigenesis in nude mice. **A**) 5-Bromodeoxyuridine (BrdU) incorporation assay. Immortalized human prostate epithelial cells (iPrECs), with or without the androgen receptor (AR) stably transfected with either the empty vector (EV) or *FASN*, were cultured for 2 days and 10 μM BrdU was added to the culture medium 1 hour before harvesting. The cells were analyzed by flow cytometry (10 000 cells per sample) to determine the percentage of cells that had incorporated BrdU. *P* values (Student *t* test) are two-sided. Mean percentage of BrdU-labeled cells in triplicate samples and 95% confidence intervals (**error bars**) are shown. **B**) Immunoblot analysis of FASN protein expression in iPrECs, AR-iPrECs, and LNCaP cells stably transfected with pBabe empty vector (**lanes 1, 3, 5**) and pBabe FASN (**lanes 2, 4, 6**). **C**) Anchorage-independent growth assay. The mean number of colonies 200 μm or greater in diameter that grew in soft agar from three independent experiments, each performed in triplicate, are plotted. AR-iPrECs and LNCaP cells are compared with the isogenic cell lines overexpressing FASN. iPrECs are also compared with iPrECs overexpressing H-ras^{Val12}. Colonies (**lower panels**) are shown at ×20 and ×100 magnification. **D**) Hematoxylin-eosin–stained sections (**upper left**) and corresponding immunohistochemistry (**brown staining**, methyl green counterstaining) for AR, FASN, and SV40-large T antigen on orthotopic tumors derived from injection of AR-iPrEC-FASN in the anterior prostate of nude mice (scale bar = 50 μm). Mouse prostate acinus is on the right (**yellow arrow, upper left panel**), whereas established tumor derived from AR-iPrEC-FASN human cells is in the stroma beneath the gland on the left (**black arrow, upper left panel**). For comparison, two-tailed Student *t* test was used.

these cells to grow subcutaneously in nude mice with substantially greater efficiency (eight of nine vs three of nine mice formed tumors) when compared with LNCaP cells transfected with the empty vector.

Taken together, these results indicate that overexpression of FASN induces transformation of and confers tumorigenicity to immortalized prostate epithelial cells.

Generation of Transgenic Mice That Express FASN in the Prostate

To examine the oncogenic role of FASN in vivo, we generated transgenic mice that expressed FASN in the prostate under the control the prostate-specific ARR2 probasin promoter. The expression construct that we used to generate these mice also included a luciferase reporter gene under the control of an IRES (Supplementary Figure 1, A, available online). Three of 11 founder mice carried the transgene, and F1 progeny from those three strains were bred for several generations. We used multiple assays to confirm the presence of the transgene: a PCR-based genotyping method that used primers located in the 3′ region of the probasin promoter and in the 5′ region of the *FASN* transgene (all mice); in vitro and in vivo luciferase assays (15/116 and 25/116 mice, respectively; Supplementary Figure 1, B, available online); FASN and luciferase immunohistochemistry (all mice, data not shown); and luciferase assays of the hemilobe of the prostate that was contralateral to the one used for histopathological analysis. In wild-type control (ie, nontransgenic) mice, we detected substantial levels of endogenous FASN protein in liver and preputial gland lysates by

immunoblotting (Supplementary Figure 1, A, available online) and in liver and preputial gland tissue by immunohistochemistry (data not shown). In *FASN*-transgenic mice, FASN protein was detected by immunohistochemistry in liver and preputial glands and in all of the prostate lobes (data not shown), with highest expression in the ventral lobe as determined by in vitro luciferase activity (Supplementary Figure 1, B, available online), immunoblotting (Supplementary Figure 1, C, available online), and by immunohistochemistry (data not shown).

Effect of Prostatic Expression of FASN in Transgenic Mice

Because forced expression of FASN in prostate epithelial cells resulted in increased proliferative activity (Supplementary Figure 1, D, available online), we first examined whether FASN overexpression resulted in hyperplasia in the mouse prostate. To do this, we paraffin embedded all of the prostate hemilobes of 146 male mice from the three founder lines (mice were aged 8 weeks to 14 months, 116 transgenics and 30 wild type) and serially sectioned each in their entirety. We recorded the largest diameter of each lobe and used it and the number of acini present in the largest diameter section of each lobe as independent measures of hyperplasia (Figure 2, C).

Histological examination of the serial sections revealed that proliferating cells filled the lumens of ventral, anterior, and dorsolateral prostate lobes (Figure 2, A). We observed macroscopic obstruction of the bladder outflow by the enlarged prostate in several older males and noted a substantial enlargement of all prostate lobes compared with age-matched, wild-type littermate

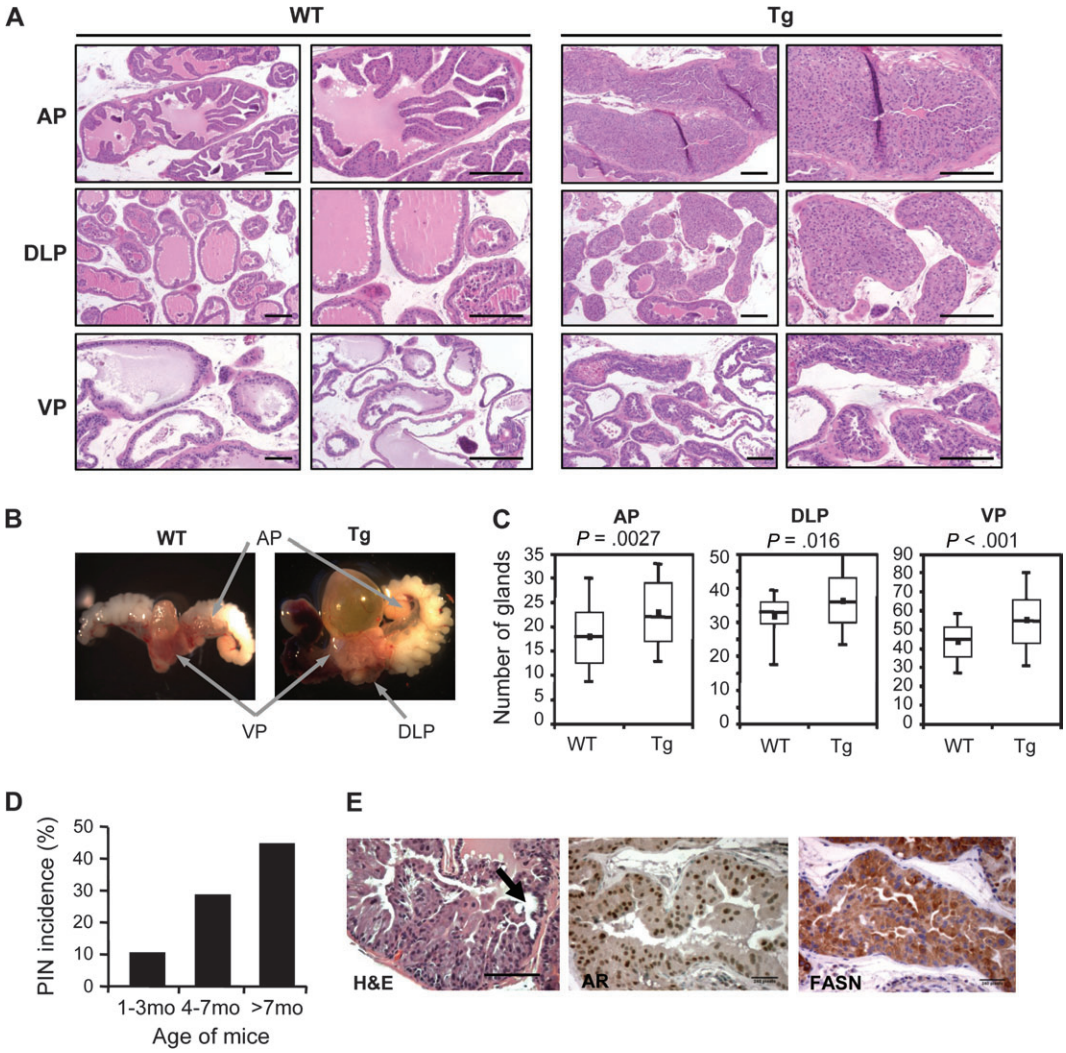

Figure 2. Phenotype of prostate-specific fatty acid synthase (*FASN*)-transgenic (Tg) mice. **A**) Representative histological images of the anterior (AP), dorsolateral (DLP), and ventral (VP) prostatic lobes of a 6-month-old *FASN*-transgenic (Tg) mouse and a wild-type (WT) mouse (scale bar = 100 μm). Epithelial hyperplasia is evident in the Tg mouse prostate (scale bar = 100 μm) as shown by the filling of glandular lumen by hyperplastic epithelial cells. **B**) Prostatic hyperplasia leading to bladder outlet obstruction and bladder distension. **C**) **Box plots** showing the number of acini per largest diameter section from all of the prostate lobes in FASN-Tg and WT mice. **Lower and higher whiskers** indicate 10th and 90th percentile, respectively; **lower and higher edges of box** indicate 25th and 75th percentile, respectively; the **inner line** in the **box** indicates 50th percentile; and the **dot** in the **box** indicates the average of all data. For comparison of WT and Tg, a two-tailed Student *t* test was used. **D**) Age-related incidence of prostate intraepithelial neoplasia (PIN) in FASN-Tg mice. Incidence of PIN in FASN-Tg mice aged 1–3, 4–7, and 7 or more months. **E**) Example of the PIN phenotype in *FASN*-transgenic mice: hematoxylin–eosin (H&E) (**arrow** shows transition from normal to neoplastic epithelium) and immunohistochemical staining for FASN and androgen receptor (scale bar=100 μm).

control mice (Figure 2, B). Finally, an antibody against the proliferation antigen Ki67 (Supplementary Figure 1, D, available online) and the number of acini present in the largest diameter section of each lobe (Figure 2, C) were used to assess the extent of hyperplasia among the prostate samples. Compared with aged-matched, littermate control mice, FASN-transgenic mice had a statistically significantly greater number of acini and higher proliferative rates in all prostatic lobes. The average numbers of acini in the largest diameter section of anterior prostates from wild-type vs *FASN*-transgenic mice were 18.0 vs 23.0 (P = .0027), in wild-type vs *FASN*-transgenic dorsolateral prostate lobes were 31.7 vs 36.3 (P = .016); the average numbers of acini in the largest diameter section of ventral prostates from wild-type vs *FASN*-transgenic were 43.9 vs 55.4 (P < .001) (Figure 2, C).

Histological examination of the serial prostate sections also revealed a second important phenotype in *FASN*-transgenic mice—PIN—that displayed low penetrance and was age dependent. We observed no PIN in prostate glands obtained from mice younger than 2 months, whereas the highest incidence of PIN was recorded in mice aged 1 year or older. The overall incidence of PIN in FASN-transgenic mice was 28% (33/116). Importantly, the incidence of PIN increased substantially with age, from 10% (95% CI = 1% to 22%) in 8- to 16-week-old mice to 39% (95% CI = 26.5% to 51.4%) in 4- to 7-month-old mice and 44% (95% CI = 26.7% to 62.9%) in mice aged 7 months to 1 year (P = .0028 when comparing group 1 to groups 2 and 3 by Fisher exact test) (Figure 2, D). Invasive prostate carcinoma was not observed in any of the mice examined. Prostate tissues obtained from *FASN*-transgenic mice were positive for FASN and AR by immunohistochemistry in all mice (data not shown) (Figure 2, E).

Together, these findings indicate that overexpression of FASN, a metabolic enzyme, in immortalized prostate cells induces invasive adenocarcinomas and that FASN-transgenic mice develop prostate hyperplasia and in situ neoplasia in vivo.

Effect of FASN Overexpression on Apoptosis

Apoptosis occurs by two major pathways: intrinsic and extrinsic. The intrinsic pathway is activated by stress inducers, such as DNA-damaging agents, which trigger the mitochondria to release factors into the cytosol that aid in caspase 9 activation. The extrinsic pathway is activated by stimulation of death receptors (ie, Fas and TRAIL), which then trimerize to form a complex that activates caspase 8. Both caspase 8 and 9 cleave and activate caspase 3 to induce DNA fragmentation, which is characteristic of apoptosis (39).

Although an antiapoptotic role for FASN was previously suggested (37,40–42), which of these pathways was inhibited was unclear. We therefore examined whether FASN could protect against apoptosis induced by agents that stimulate the intrinsic and the extrinsic pathways. We treated iPrECs and iPrEC-FASN cells with camptothecin, a stimulator of the intrinsic pathway, or anti-Fas antibody, a stimulator of the extrinsic pathway, for 20 hours. Because anti-Fas antibody treatment alone had a minimal effect on apoptosis in iPrECs, we also treated these cells with anti-Fas antibodies and cycloheximide, which was added to enhance death receptor signaling, as previously described (43). The cells were harvested and evaluated for DNA fragmentation, an early marker of apoptosis, by PI staining and flow cytometry analysis. Camptothecin (as well as etoposide, another intrinsic pathway stimulator; data not shown) induced statistically significantly less apoptosis in iPrECs and LNCaP cells that overexpressed FASN than in cognate cells that expressed empty vector (mean percentage of apoptotic iPrECs per well after 20 hours of 50 nM camptothecin, empty vector vs FASN: 31.9% vs 19.5%, difference = 12.4%, 95% CI = 1.6% to 23.2%, P = .033 [Figure 3, A]; mean percentage of apoptotic LNCaP cells per well after 20 hours of 50 nM camptothecin, empty vector vs FASN: 15.5% vs 6.5%, difference = 8.9%, 95% CI = 2% to 15.9%, P = .023 [Figure 3, B]). By contrast, there was no statistically significant difference in apoptosis levels between iPrECs and iPrEC-FASN cells treated with 100 or 500 ng/mL anti-Fas antibody (Figure 3, C). These results indicate that FASN overexpression protects immortalized prostate epithelial cells from mitochondria-mediated apoptosis (ie, the intrinsic pathway) but is ineffective at regulating apoptosis via death receptor stimulation (ie, the extrinsic pathway).

Apoptosis-inducing agents that target mitochondria often cause a decrease in mitochondrial membrane potential that precedes the release of mitochondrial proapoptotic factors (44). We therefore examined the effect of camptothecin on mitochondrial membrane potential in iPrECs. iPrEC-EV and iPrEC-FASN cells were incubated with camptothecin for 18 hours and then stained with rhodamine 123 dye, which is incorporated into cells in proportion to their mitochondrial membrane potentials. Whereas rhodamine incorporation among camptothecin-treated iPrEC-EV cells decreased 26.8% relative to untreated cells, reflecting a collapse in mitochondrial membrane potential, rhodamine incorporation in PrEC-FASN cells that were incubated for 18 hours in camptothecin decreased by only 1.9% relative to untreated cells (Figure 3, D). These data suggest that FASN is important in preserving mitochondrial membrane potential and that it may thus be involved in inhibiting camptothecin-induced cell death.

Effect of siRNA-Mediated *FASN* Silencing on Apoptosis in LNCaP Cells

Because overexpression of FASN protected immortalized prostate epithelial cells from apoptosis induced by genotoxic agents such as camptothecin and etoposide, we next wanted to assess the effect of short interfering RNA to *FASN* on apoptosis in prostate androgen-dependent tumor cells (LNCaP). To accomplish this, LNCaP cells were transfected with FASN siRNA, and apoptosis was measured daily up to 120 hours after transfection by Hoechst staining. LNCaP cells displayed a substantial level of apoptosis by 72 hours after transfection, with the maximum level of apoptosis observed by 120 hours after transfection (at 24 hours after transfection, 1.2% apoptotic cells with scrambled-sequence siRNA vs 1.9% apoptotic cells with FASN siRNA, difference = 1.3%, 95% CI = −0.1% to 1.4%, P = .09; at 48 hours after transfection, 1.7% vs 4.5%, difference = 2.9%, 95% CI = 1.6% to 4.1%, P = .0014; at 72 hours after transfection, 1.7% vs 24.1%, difference = 22.5%, 95% CI = 19.3% to 25.6%, P < .001; at 96 hours after transfection, 3.3% vs 72.3%, difference = 69.0%, 95% CI = 63.4% to 74.6%, P < .001; at 120 hours after transfection, 3.2% vs 89.1%, difference = 85.8%, 95% CI = 78.6% to 93.0%, P < .001) (Figure 3, E, left panel). Protein lysates generated from these cells were also subjected to immunoblot analysis of PARP cleavage, which is indicative of apoptosis.

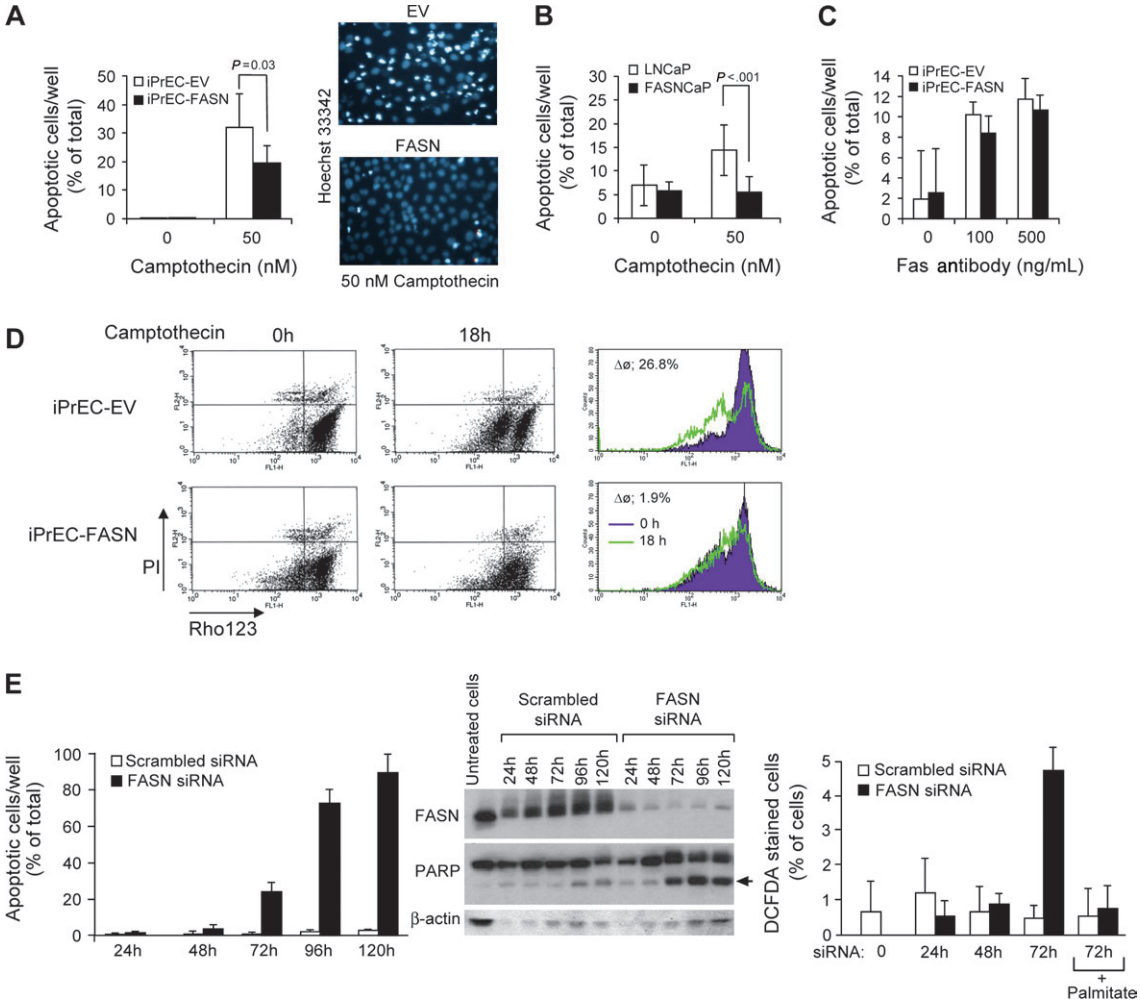

Figure 3. Effect of fatty acid synthase (FASN) overexpression on apoptosis. **A**) Apoptotic cell percentage (**left bar graph**) after Hoechst 33342 staining (**right panels**: strong **white signals** indicate apoptotic cells) of immortalized human prostate epithelial cells–empty vector (iPrEC-EV) and iPrEC-FASN cells treated with 50 nM camptothecin, a stimulator of mitochondria-mediated apoptosis. **B**) Percentage of apoptosis among LNCaP-EV and FASNCaP cells after treatment with 50 nM camptothecin as measured by Hoechst 33342 staining. **C**) Percentage of apoptosis in iPrEC-EV and iPrEC-FASN cells following treatment with 100–500 ng/mL of an antibody activating Fas, a proapoptotic tumor necrosis factor family cell surface receptor. Mean values of triplicate samples and 95% confidence intervals (CIs) from three independent experiments are shown; *P* values are from two-sided Student *t* tests. **D**) Mitochondrial membrane potential changes ($\Delta\Psi$) after treatment of iPrEC-EV and iPrEC-FASN cells with 50 nM camptothecin as assessed by rhodamine 123 (Rho 123) incorporation. A representative experiment is shown as **dot plots** (**left**) and histograms (**right**: 0 hours in **purple**, 18 hours in **green**). Viability was assessed by propidium iodide (PI) staining. **E**) Percentage of apoptosis (**left bar graph**) induced by treatment of LNCaP cells with 20 nM anti-FASN small interfering RNA (siRNA) at 24-hour intervals from 24 to 120 hours. Cleaved poly (ADP-ribose) polymerase expression as a measure of apoptosis was detected by immunoblot (**middle panel, arrow**). Reactive oxygen species (ROS) production in LNCaP cells treated with anti-FASN siRNA and palmitate (**right panel**). ROS production was determined by carboxy-H_2DCFDA staining using flow cytometry.

Whereas no dramatic increase in PARP cleavage was detectable in cells transfected with scrambled-sequence control siRNA, cells transfected with FASN siRNA exhibited a substantial increase in PARP cleavage beginning at 72 hours after transfection (Figure 3, E, middle panel, lower band for cleaved PARP).

Mitochondria generate substantial amounts of ROS, including hydroxyl radicals and superoxide anions. High levels of intracellular ROS cause substantial damage to cells through membrane lipid peroxidation or through the activation of apoptotic pathways. To examine whether FASN affected ROS generation, we used a fluorescent indicator of intracellular ROS, carboxy-H_2DCFDA, in iPrEC-EV and iPrEC-FASN cells that were treated with siRNA against FASN and with the mitochondrial genotoxic agents camptothecin and etoposide. We found that ROS generation in iPrEC-EV cells increased in a dose-dependent manner but was substantially attenuated in iPrEC-FASN cells (data not shown).

Importantly, the addition of 100 μM palmitate, the enzymatic product of FASN, to the growth medium of LNCaP cells completely abolished the increase in the intracellular generation of ROS induced by siRNA-mediated silencing of *FASN* at 72 hours following treatment (Figure 3, E, right panel). These observations strongly suggest that *FASN* knockdown–mediated apoptosis may be a result of a decrease in palmitate production.

Effect of FASN Expression on Castration-Mediated Apoptosis In Vivo

We next examined whether FASN overexpression would have an antiapoptotic effect in vivo by using four *FASN*-transgenic mice

and four wild-type, age-matched (4-month-old) control mice that had been castrated to eliminate the source of androgens. The goal was to assess the apoptotic rate in prostate epithelial cells at a time when the FASN transgene was still expressed (as measured by in vivo luciferase bioluminescence resulting from FASN and luciferase co-expression driven by the androgen-responsive promoter; Supplementary Figure 1, available online) and when castration-related cell death was known to occur. By 3 days after castration, luciferase bioluminescence signals reflecting transgene expression were still detectable in the *FASN*-transgenic mice, albeit at decreased levels compared with castrated aged-matched control mice (Figure 4, A and B). By 3 days after castration, the number of apoptotic cells relative to viable epithelial cells in the ventral lobe of the prostate of wild-type mice increased substantially (Figure 4, C, iii), whereas the number of apoptotic cells in FASN-transgenic mice did not (Figure 4, C, iv), likely because FASN levels in the *FASN*-transgenic mice were still high (Figure 4, C, x). At 7 days after castration, when the activity of the probasin promoter and thus the expression of the *FASN* transgene was completely abolished due to suppression of androgen production as a result of castration, apoptotic levels were high in both wild-type and *FASN*-transgenic mice (Figure 4, C, v, vi). Variations in the apoptotic rate and FASN intensity at time zero (before castration) and at day 3 and day 7 after castration in wild-type and *FASN*-transgenic mice are summarized in Figure 4, D (apoptotic rate in wild-type vs transgenic mice at 3 days after castration: 14% vs 4.5%, difference = 9.5%, 95% CI = 6.8% to 12.2%, $P < .001$). To our knowledge, this is the first in vivo demonstration that FASN protects prostate epithelial cells from castration-induced apoptosis.

Correlation Between FASN Overexpression Apoptosis in Human Prostate Cancer

Finally, we assessed the correlation between FASN expression and apoptosis in human prostate cancer tissues by subjecting TMAs that included tumor specimens from 745 men with prostate cancer to immunohistochemical analysis of FASN expression and to the terminal deoxynucleotidyltransferase-mediated UTP end-labeling (TUNEL; Apoptag) assay to detect apoptotic cells (Figure 5, A). We categorized the tumor samples into four groups (quartiles) based on their expression of FASN and compared the percentage of TUNEL-positive (ie, apoptotic) cells in each group. The Pearson correlation coefficient between log-transformed apoptotic rate and quartiles of FASN expression was −.11 (95% CI = −.18 to −.04, $P = .002$). We found that the log-transformed percentage of TUNEL-positive cells decreased with increasing quartile of FASN expression in the tumors. Compared with tumors in the lowest quartile of FASN expression, those in the highest quartile of FASN expression had 51% fewer TUNEL-positive cells (mean percentage of apoptotic cells, lowest vs highest quartile of FASN expression: 2.76 vs 1.34, difference = 1.41, 95% CI = 0.45 to 2.39, $P_{trend} = .0046$) (Figure 5, B). These data suggest that FASN overexpression exerts an antiapoptotic effect in human prostate cancer.

Discussion

In this paper we show that forced overexpression of a metabolic enzyme—FASN—together with expression of the AR in prostate epithelial cells facilitates the development of invasive cancers when these cells are injected orthotopically into mice and results in age-dependent PIN when expressed as a transgene in the murine prostate. We also show that FASN exerts its oncogenic effects at least in part by protecting prostate epithelial cells from apoptosis in transgenic mice and in a large series of human prostate cancers.

Prostate cancer is a leading cause of male cancer-related death, second only to lung cancer, and represents about 10% of all cancer deaths among men in the United States (45). Dietary and lifestyle factors appear to be important risk factors for prostate cancer mortality; specifically, higher body mass index and adult weight gain are associated with an increased risk of dying from prostate cancer (20–29). Dietary intervention or regulation of metabolic pathways may therefore potentially affect prostate cancer incidence and, perhaps, tumor aggressiveness.

FASN catalyzes the synthesis of palmitate from the condensation of malonyl-CoA and acetyl-CoA and plays an important role in energy homeostasis by converting excess carbon intake into fatty acids for storage. It has been shown that FASN expression is markedly increased in several human malignancies, notably breast and prostate cancer, and its overexpression in tumor tissues from patients with colon, breast, and prostate carcinomas as well as melanoma and gastrointestinal stromal tumors has been associated with a poor prognosis (3–12). In addition, one-fourth of human prostate cancers have genomic amplification of *FASN* (13). Despite these clinical association studies, to our knowledge, there has been no bona fide demonstration of *FASN* oncogenicity in cultured cells or in vivo. To this end, we have demonstrated that forced overexpression of *FASN* in immortalized prostate epithelial cells results in transformation of immortalized epithelial cells and in tumor formation in vivo. More importantly, when expressed as a transgene in mice, *FASN* was associated with the development of prostate epithelial hyperplasia and intraepithelial neoplasia. Taken together with the previous evidence of FASN overexpression and/or of *FASN* gene amplification in prostate cancer, these data provide the first evidence to our knowledge that the mere overexpression of a metabolic enzyme can result in neoplastic transformation of epithelial cells.

The biochemical and metabolic basis, as well as the biological consequences, of FASN overexpression are not well understood. The antiproliferative and proapoptotic effects of FASN inhibition have been shown in several systems (40,46–48). In addition, functional interference, mostly by RNA interference, of enzymes that precede FASN in the fatty acid synthetic pathway, such as ATP citrate lyase and acetyl-CoA carboxylase, has been shown to result in G_1 arrest and/or induction of apoptosis (49–51). The reported induction of programmed cell death through FASN blockade in other studies led us to investigate inhibition of apoptosis as the predominant mechanism of oncogenic action of FASN in this study. We showed that *FASN* overexpression protected cells from apoptosis via stabilization of mitochondrial membrane potential but had no effect on the extrinsic apoptotic cascade that involves Fas and Fas ligand. Importantly, we showed that castration-induced apoptosis was statistically significantly inhibited in *FASN*-transgenic mice. Furthermore, the increase in ROS that resulted from treatment of LNCaP cells with FASN siRNA was reversed by supplying palmitate, the principal enzymatic product of FASN, to the culture media, suggesting that the products of de novo

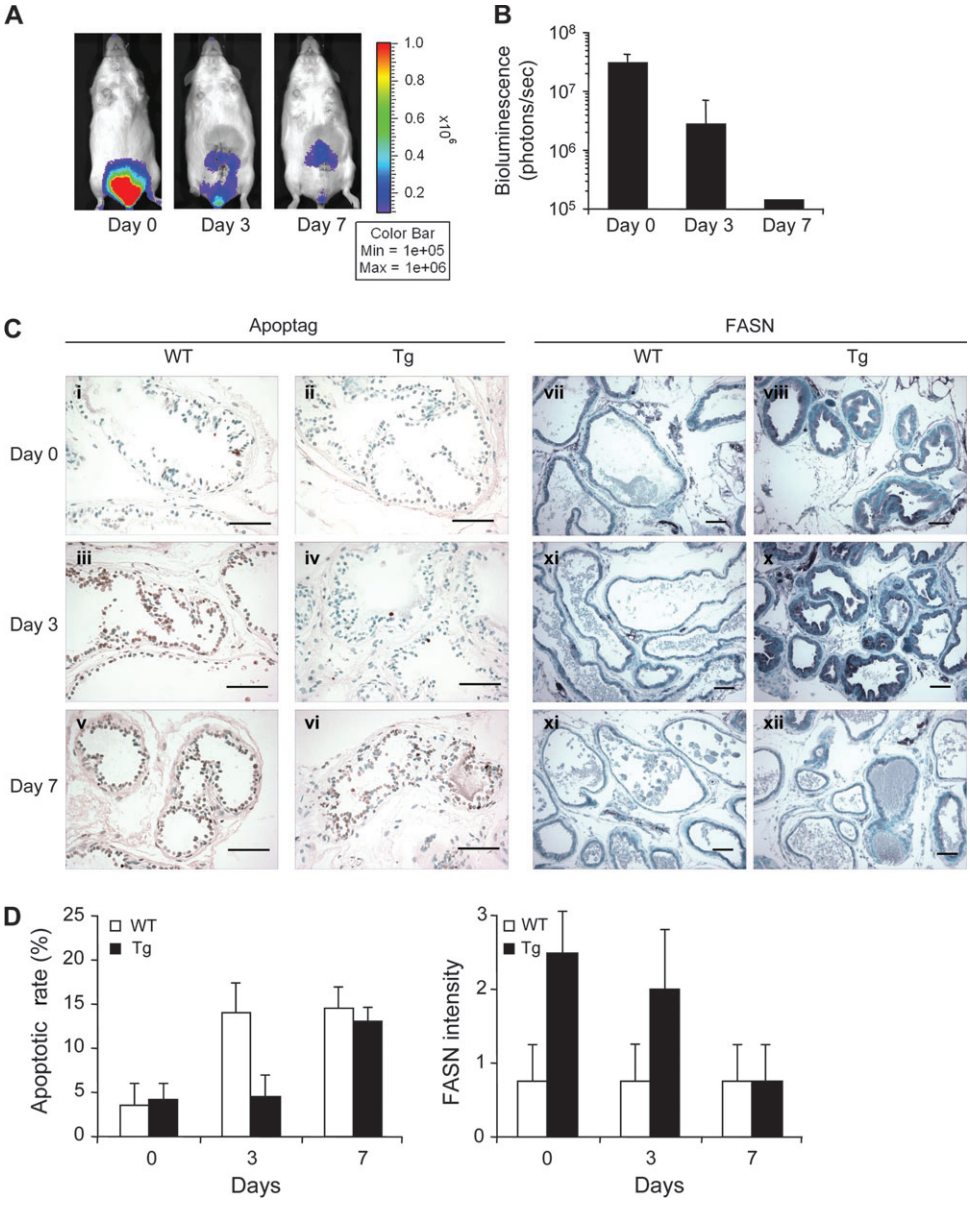

Figure 4. Bioluminescence imaging of fatty acid synthase (FASN)-transgenic (Tg) mice 0, 3, and 7 days after castration. To demonstrate the decrease in expression of the transgene as measured by luciferase activity in the prostate of Tg mice after castration, in vivo images were acquired at day 0, 3, and 7 after injection of D-luciferin (150 mg/kg body weight) via the tail vein. Pseudocolor images represent intensity of emitted light (**red** most intense and **blue** least intense). **B**) Signal intensity of luciferase activity in (**A**) as measured by photon counts. **C**) Terminal deoxynucleotidyltransferase-mediated UTP end-labeling (Apoptag) assay on ventral prostate tissue showing apoptotic cells by brown nuclear staining, counterstained with methyl green (wild type [WT] and Tg at 0, 3 and 7 days; first two columns on the **left**). FASN immunohistochemistry in sections of ventral prostate showing cytoplasmic FASN expression in blue counterstained with methyl green (WT and Tg at 0, 3 and 7 days; two columns on **right**). Ventral prostate sections from one representative WT and Tg mouse are shown. **D**) Percentage of apoptotic epithelial cells as compared with total cells (left) and FASN expression (right) in ventral prostate tissue by semiquantitative analysis of at least four high-power fields or 1000 cells per mouse (*P* value from two-tailed Student *t* test).

FASN synthesis, such as palmitate, may alter mitochondrial membranes and protect LNCaP cells from diffusion of ROS to outside the mitochondria. Phospholipids, the end product of nearly 85% of all lipids synthesized de novo by FASN in tumor cells, have been observed to end up in lipid rafts in plasma membranes (52). Therefore, general alterations in the lipid compositions of the cellular and mitochondrial membranes may confer a selective growth advantage to cells that display increased FASN activity by inhibition of apoptosis. We previously reported (53) that human prostate adenocarcinomas with the lowest expression of USP2a, an isopeptidase that stabilizes and prolongs the half-life of FASN (16), also had the lowest expression of FASN and were specifically and statistically significantly associated with a cell death gene set when tested against 440 predetermined gene sets by a gene-set enrichment analysis (16). These data together with the reciprocal correlation between low FASN expression and high apoptosis that we report here further support an inverse association between FASN levels and proapoptotic gene expression.

The transition from an androgen-dependent status to androgen independence is the key feature of lethal prostate cancers. Hormone resistance occurs as a result of a diminished apoptotic response to castration, resulting in androgen-independent disease. In addition, anticancer therapeutic regimens, including chemotherapy, radiation therapy, and immunotherapy also trigger tumor cell death through the induction of apoptosis. We showed that overexpression of FASN protein in immortalized or transformed prostate epithelial cells, which in clinical samples occurs predominantly in castration-resistant disease metastatic to bone (7), results in resistance to apoptosis induced by chemotherapeutic regimens. Importantly, we also showed that a strong and inverse relationship exists between FASN expression and apoptosis measured by DNA fragmentation assays in a large cohort of prostate cancer patients, as was previously suggested in more limited series of patients (54,55).

The experimental evidence we provide on the oncogenic role of FASN in the prostate suggests that pharmacological targeting

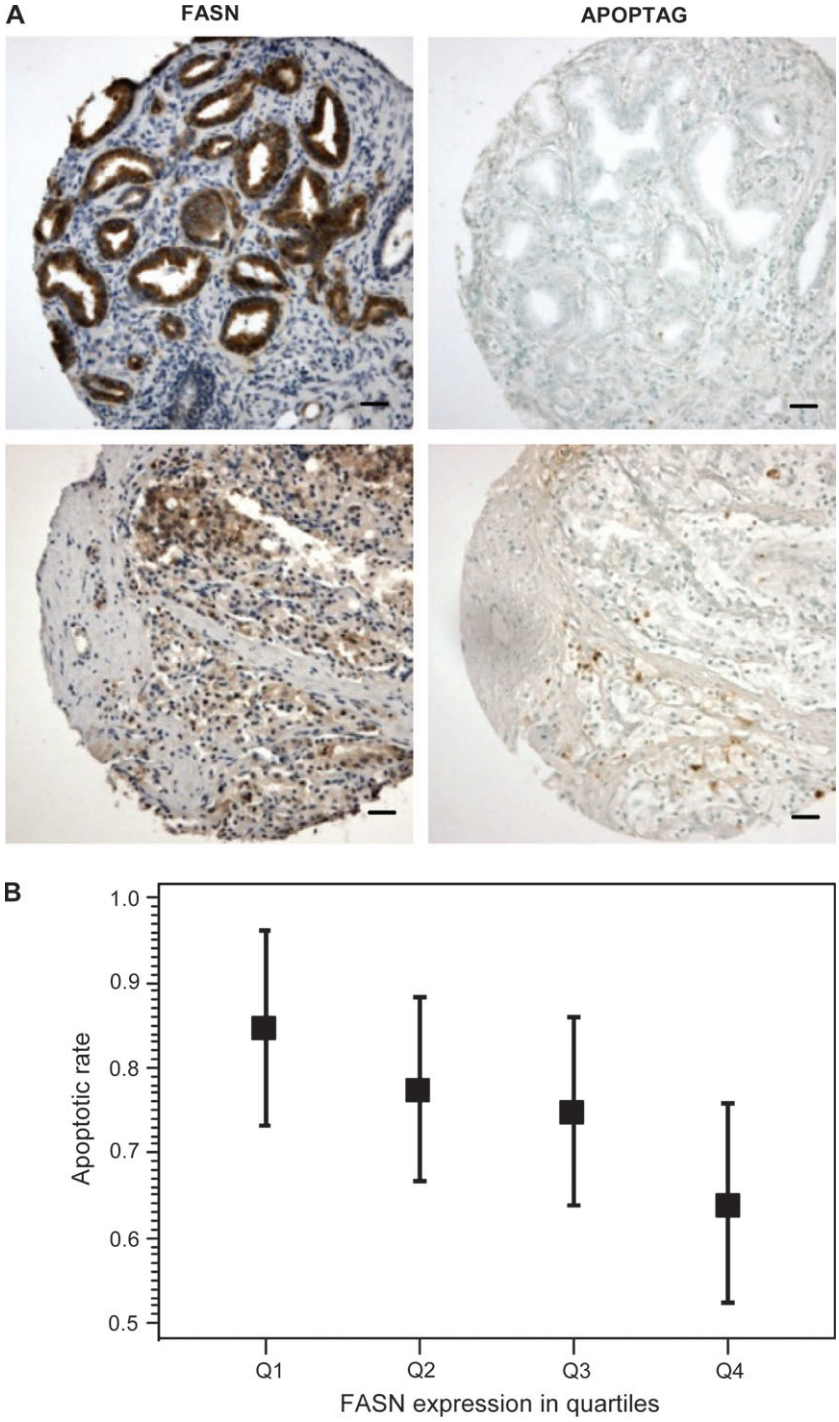

Figure 5. Association between apoptotic rate and fatty acid synthase (FASN) expression in human prostate cancer. **A**) Representative images of FASN immunoexpression levels (**left panels**) and apoptosis (Apoptag; **right panels**) in human prostate cancer tissue microarray with high (**top left**) or low (**bottom left**) FASN expression (scale bar = 100 μm). **B**) Statistically significant inverse association between FASN expression in 745 prostate tumor samples (categorized by quartiles of FASN expression) and apoptotic rate (P_{trend} = .0046).

of FASN might represent an effective treatment for prostate cancer. The recent description of the crystal structure of a mammalian FASN revealed an important opportunity for the discovery of new FASN-targeting drugs (56). FASN inhibitors, such as C75 (α-methylene-γ-butyrolactone), the mycotoxin cerulenin, and their derivatives induce apoptosis in several types of cancer cells including prostate, breast, sarcoma, and melanoma and decrease the size of prostate cancer xenografts and autochthonous tumors that overexpress FASN (57). Orlistat, an antiobesity drug approved by the Food and Drug Administration, induces apoptosis in FASN-overexpressing prostate tumors by inhibiting the thioesterase domain of FASN (15). More recent discoveries include the novel drug GSK837149A (58) and new beta-lactone inhibitors (59), which target the β-ketoacyl reductase and the thioesterase domains of FASN, respectively. These advances, taken together with our data on FASN oncogenicity, suggest that pharmacological targeting of FASN may be a possible and effective means of preventing prostatic tumorigenesis as well as tumor maintenance in prostate cancers that overexpress this enzyme.

The data we show provide only a preliminary and limited explanation for the undoubtedly complex function of FASN and for the consequences of the induction of the lipogenic phenotype in prostate epithelial transformation. Specifically, the antiapoptotic activity of FASN reported here represents perhaps just one of many potential mechanisms of FASN-mediated oncogenicity. For example, increased production of fatty acids, particularly palmitate, in prostate tumor cells may result in the activation through palmitoylation of various cell signaling–related proteins such as such as, RAS, mitogen-activated protein kinases, and Wnt . Our study was limited to the antiapoptotic function of FASN. Another limitation of our study that deserves further investigation is that the models we used did not address the role played by lipid-modifying enzymes such as desaturases on FASN enzymatic products, specifically palmitate. These modifications may play an important role in alterations in cellular and mitochondrial membranes, and in turn would affect signaling and apoptotic response in cells that overexpress FASN. Finally, overexpression of *FASN* as a transgene did not result in invasive adenocarcinomas. Development of age-dependent PIN but not invasive cancer in our *FASN*-transgenic mouse model indicates that although increased expression of FASN is able to transform prostate cells, it is not sufficient to induce invasive prostate cancer. *FASN* has indeed been found to be amplified in prostatic adenocarcinomas (13) and overexpression of FASN protein is associated with higher stage and grade (7), suggesting that it plays a role in prostatic tumorigenesis. However, further studies are required to precisely identify the potential additional mechanisms of action through which FASN overexpression confers oncogenicity in the prostate.

In summary, we provide evidence that *FASN*, which encodes a metabolic enzyme and is overexpressed in many human tumors, is a bona fide oncogene in prostate cancer that exerts its oncogenic effect, at least in part, by inhibiting the intrinsic pathway of apoptosis. The identification of FASN-overexpressing tumors, which can be achieved in vivo by monitoring ^{11}C acetate uptake (60), may thus provide prognostic and biologically relevant information in patients with advanced prostate cancer. Furthermore, we speculate that a high-fat diet and obesity may also represent a permissive background for the development of a lipogenic phenotype leading to neoplastic transformation in the prostate cancer as they do in breast cancer (10), although data to support this possibility are lacking. More importantly, however, we suggest that FASN-overexpressing tumors may be resistant to chemotherapeutic agents that induce apoptosis and that inhibition of the *FASN* gene or protein should be considered as a therapeutic strategy in prostate cancer.

References

1. Medes G, Thomas A, Weinhouse S. Metabolism of neoplastic tissue. IV. A study of lipid synthesis in neoplastic tissue slices in vitro. *Cancer Res.* 1953;13(1):27–29.
2. Kusakabe T, Maeda M, Hoshi N, et al. Fatty acid synthase is expressed mainly in adult hormone-sensitive cells or cells with high lipid metabolism and in proliferating fetal cells. *J Histochem Cytochem.* 2000;48(5):613–622.
3. Shurbaji MS, Kalbfleisch JH, Thurmond TS. Immunohistochemical detection of a fatty acid synthase (OA-519) as a predictor of progression of prostate cancer. *Hum Pathol.* 1996;27(9):917–921.
4. Alo' PL, Visca P, Marci A, Mangoni A, Botti C, Di Tondo U. Expression of fatty acid synthase (FAS) as a predictor of recurrence in stage I breast carcinoma patients. *Cancer.* 1996;77(3):474–482.
5. Gansler TS, Hardman W 3rd, Hunt DA, Schaffel S, Hennigar RA. Increased expression of fatty acid synthase (OA-519) in ovarian neoplasms predicts shorter survival. *Hum Pathol.* 1997;28(6):686–692.
6. Takahiro T, Shinichi K, Toshimitsu S. Expression of fatty acid synthase as a prognostic indicator in soft tissue sarcomas. *Clin Cancer Res.* 2003;9(6):2204–2212.
7. Rossi S, Graner E, Febbo P, et al. Fatty acid synthase expression defines distinct molecular signatures in prostate cancer. *Mol Cancer Res.* 2003;1(10):707–715.
8. Visca P, Sebastiani V, Botti C, et al. Fatty acid synthase (FAS) is a marker of increased risk of recurrence in lung carcinoma. *Anticancer Res.* 2004;24(6):4169–4173.
9. Van de Sande T, Roskams T, Lerut E, et al. High-level expression of fatty acid synthase in human prostate cancer tissues is linked to activation and nuclear localization of Akt/PKB. *J Pathol.* 2005;206(2):214–219.
10. Menendez JA, Lupu R. Fatty acid synthase and the lipogenic phenotype in cancer pathogenesis. *Nat Rev Cancer.* 2007;7(10):763–777.
11. Rossi S, Ou W, Tang D, et al. Gastrointestinal stromal tumours overexpress fatty acid synthase. *J Pathol.* 2006;209(3):369–375.
12. Carvalho MA, Zecchin KG, Seguin F, et al. Fatty acid synthase inhibition with Orlistat promotes apoptosis and reduces cell growth and lymph node metastasis in a mouse melanoma model. *Int J Cancer.* 2008;123(11):2557–2565.
13. Shah US, Dhir R, Gollin SM, et al. Fatty acid synthase gene overexpression and copy number gain in prostate adenocarcinoma. *Hum Pathol.* 2006;37(4):401–409.
14. De Schrijver E, Brusselmans K, Heyns W, Verhoeven G, Swinnen JV. RNA interference-mediated silencing of the fatty acid synthase gene attenuates growth and induces morphological changes and apoptosis of LNCaP prostate cancer cells. *Cancer Res.* 2003;63(13):3799–3804.
15. Kridel SJ, Axelrod F, Rozenkrantz N, Smith JW. Orlistat is a novel inhibitor of fatty acid synthase with antitumor activity. *Cancer Res.* 2004;64(6):2070–2075.
16. Graner E, Tang D, Rossi S, et al. The isopeptidase USP2a regulates the stability of fatty acid synthase in prostate cancer. *Cancer Cell.* 2004;5(3):253–261.
17. Rubin MA, De Marzo AM. Molecular genetics of human prostate cancer. *Mod Pathol.* 2004;17(3):380–388.
18. Tomlins SA, Rhodes DR, Perner S, et al. Recurrent fusion of TMPRSS2 and ETS transcription factor genes in prostate cancer. *Science.* 2005;310(5748):644–688.
19. Eeles RA, Kote-Jarai Z, Giles GG, et al. Multiple newly identified loci associated with prostate cancer susceptibility. *Nat Genet.* 2008;40(3):316–321.
20. Andersson SO, Wolk A, Bergström R, et al. Body size and prostate cancer: a 20-year follow-up study among 135006 Swedish construction workers. *J Natl Cancer Inst.* 1997;89(5):385–389.
21. Cerhan JR, Torner JC, Lynch CF, et al. Association of smoking, body mass, and physical activity with risk of prostate cancer in the Iowa 65+ Rural Health Study (United States). *Cancer Causes Control.* 1997;8(2):229–238.
22. Engeland A, Tretli S, Bjørge T. Height, body mass index, and prostate cancer: a follow-up of 950000 Norwegian men. *Br J Cancer.* 2003;89(7):1237–1242.
23. Calle EE, Rodriguez C, Walker-Thurmond K, Thun MJ. Overweight, obesity, and mortality from cancer in a prospectively studied cohort of U.S. adults. *N Engl J Med.* 2003;348(17):1625–1638.
24. Chan JM, Gann PH, Giovannucci EL. Role of diet in prostate cancer development and progression. *J Clin Oncol.* 2005;23(32):8152–8160.
25. Gong Z, Neuhouser ML, Goodman PJ, et al. Obesity, diabetes, and risk of prostate cancer: results from the prostate cancer prevention trial. *Cancer Epidemiol Biomarkers Prev.* 2006;15(10):1977–1983.
26. Baillargeon J, Rose DP. Obesity, adipokines, and prostate cancer (review). *Int J Oncol.* 2006;28(3):737–745.
27. Wright ME, Chang SC, Schatzkin A, et al. Prospective study of adiposity and weight change in relation to prostate cancer incidence and mortality. *Cancer.* 2007;109(4):675–684.
28. Rodriguez C, Freedland SJ, Deka A, et al. Body mass index, weight change, and risk of prostate cancer in the Cancer Prevention Study II Nutrition Cohort. *Cancer Epidemiol Biomarkers Prev.* 2007;16(1):63–69.

29. Ma J, Li H, Giovannucci E, et al. Prediagnostic body-mass index, plasma C-peptide concentration, and prostate cancer-specific mortality in men with prostate cancer: a long-term survival analysis. *Lancet Oncol.* 2008; 9(11):1039–1047
30. Kuhajda FP, Jenner K, Wood FD, et al. Fatty acid synthesis: a potential selective target for antineoplastic therapy. *Proc Natl Acad Sci USA.* 1994; 91(14):6379–6383.
31. Pizer ES, Wood FD, Pasternack GR, Kuhajda FP. Fatty acid synthase (FAS): a target for cytotoxic antimetabolites in HL60 promyelocytic leukemia cells. *Cancer Res.* 1996;56(4):745–751.
32. Baron A, Migita T, Tang D, Loda M. Fatty acid synthase: a metabolic oncogene in prostate cancer? *J Cell Biochem.* 2004;91(1):47–53.
33. Berger R, Febbo PG, Majumder PK, et al. Androgen-induced differentiation and tumorigenicity of human prostate epithelial cells. *Cancer Res.* 2004;64(24):8867–8875.
34. Sesso HD, Buring JE, Christen WG, et al. Vitamins E and C in the prevention of cardiovascular disease in men: the Physicians' health study II randomized controlled trial. *JAMA.* 2008;12 300(18):2123–2133.
35. Hennekens CH, Eberlein K. A randomized trial of aspirin and beta-carotene among U.S. physicians. *Prev Med.* 1985;14(2):165–168.
36. Rimm EB, Giovannucci EL, Willett WC, et al. Prospective study of alcohol consumption and risk of coronary disease in men. *Lancet.* 1991; 338(8765):464–468.
37. Riedl SJ, Salvesen GS. The apoptosome: signaling platform of cell death. *Nat Rev Mol Cell Biol.* 2007;8(5):405–413.
38. Pagano M, Gauvreau K. Multiple regression. In: Carolyn Crockett, ed. *Principles of Biostatistics.* 2nd ed. Pacific Grove, CA: Duxbury Press Publisher, 2000;446–449.
39. Schmidt LJ, Ballman KV, Tindall DJ. Inhibition of fatty acid synthase activity in prostate cancer cells by dutasteride. *Prostate.* 2007;67(10): 1111–1120.
40. Furuta E, Pai SK, Zhan R, et al. Fatty acid synthase gene is up-regulated by hypoxia via activation of Akt and sterol regulatory element binding protein-1. *Cancer Res.* 2008;68(4):1003–1011.
41. Liu H, Liu Y, Zhang JT. A new mechanism of drug resistance in breast cancer cells: fatty acid synthase overexpression-mediated palmitate overproduction. *Mol Cancer Ther.* 2008;7(2):263–270.
42. Vazquez-Martin A, Colomer R, Brunet J, Lupu R, Menendez JA. Overexpression of fatty acid synthase gene activates HER1/HER2 tyrosine kinase receptors in human breast epithelial cells. *Cell Prolif.* 2008; 41(1):59–85.
43. Yonehara S, Ishii A, Yonehara M. A cell-killing monoclonal antibody (anti-Fas) to a cell surface antigen co-downregulated with the receptor of tumor necrosis factor. *J Exp Med.* 1989;169(5):1747–1756.
44. Kroemer G, Reed JC. Mitochondrial control of cell death. *Nat Med.* 2000;6(6):513–519.
45. Albertsen PC, Hanley JA, Fine J. 20-year outcomes following conservative management of clinically localized prostate cancer. *JAMA.* 2005;293(17): 2095–2101.
46. Furuya Y, Akimoto S, Yasuda K, Ito H. Apoptosis of androgen-independent prostate cell line induced by inhibition of fatty acid synthesis. *Anticancer Res.* 1997;17(6D):4589–4593.
47. Pizer ES, Chrest FJ, DiGiuseppe JA, Han WF. Pharmacological inhibitors of mammalian fatty acid synthase suppress DNA replication and induce apoptosis in tumor cell lines. *Cancer Res.* 1998;58(20): 4611–4615.
48. Li JN, Gorospe M, Chrest FJ, et al. Pharmacological inhibition of fatty acid synthase activity produces both cytostatic and cytotoxic effects modulated by p53. *Cancer Res.* 2001;61(4):1493–1499.
49. Hatzivassiliou G, Zhao F, Bauer DE, et al. ATP citrate lyase inhibition can suppress tumor cell growth. *Cancer Cell.* 2005;8(4):311–321.
50. Beckers A, Organe S, Timmermans L, et al. Chemical inhibition of acetyl-CoA carboxylase induces growth arrest and cytotoxicity selectively in cancer cells. *Cancer Res.* 2007;67(17):8180–8187.
51. Brusselmans K, De Schrijver E, Verhoeven G, Swinnen JV. RNA interference-mediated silencing of the acetyl-CoA-carboxylase-alpha gene induces growth inhibition and apoptosis of prostate cancer cells. *Cancer Res.* 2005;65(15):6719–6725.
52. Swinnen JV, Van Veldhoven PP, Timmermans L, et al. Fatty acid synthase drives the synthesis of phospholipids partitioning into detergent-resistant membrane microdomains. *Biochem Biophys Res Commun.* 2003;302(4): 898–903.
53. Priolo C, Tang D, Brahamandan M, et al. The isopeptidase USP2a protects human prostate cancer from apoptosis. *Cancer Res.* 2006;66(17): 8625–8632.
54. Huang X, Zhang X, Farahvash B, Olumi AF. Novel targeted pro-apoptotic agents for the treatment of prostate cancer. *J Urol.* 2007;178(5):1846–1854.
55. Uzzo RG, Haas NB, Crispen PL, Kolenko VM. Mechanisms of apoptosis resistance and treatment strategies to overcome them in hormone-refractory prostate cancer. *Cancer.* 2008;112(8):1660–1671.
56. Maier T, Leibundgut M, Ban N. The crystal structure of a mammalian fatty acid synthase. *Science.* 2008;321(5894):1315–1322.
57. Kuhajda FP, Pizer ES, Li JN, Mani NS, Frehywot GL, Townsend CA. Synthesis and antitumor activity of an inhibitor of fatty acid synthase. *Proc Natl Acad Sci USA.* 2000;97(7):3450–3454.
58. Vázquez MJ, Leavens W, Liu R, et al. Discovery of GSK837149A, an inhibitor of human fatty acid synthase targeting the beta-ketoacyl reductase reaction. *FEBS J.* 2008;275(7):1556–1567.
59. Richardson RD, Ma G, Oyola Y, et al. Synthesis of novel beta-lactone inhibitors of fatty acid synthase. *J Med Chem.* 2008;51(17):5285–5296.
60. Vāvere AL, Kridel SJ, Wheeler FB, Lewis JS. 1-11C-acetate as a PET radiopharmaceutical for imaging fatty acid synthase expression in prostate cancer. *J Nucl Med.* 2008;49(2):327–334.

Funding

Support for this work (to M.L.) was obtained from the Prostate Cancer Foundation, the National Cancer Institute (RO1CA131945, PO1CA89021, P50 CA90381, and CA55075), Dana Farber Cancer Institute-Novartis Drug Development Program, the Linda and Arthur Gelb Center for Translational Research, a gift from Nuclea Biomarkers to the Jimmy Fund and the Loda laboratory, and the Samuel Waxman Foundation (SPA P01-Waxman-CS01). E.P. and G.Z. are supported by a fellowship of the American–Italian Cancer Foundation.

Notes

The authors are grateful to Anna Eisenstein and Jennifer Anne Sinnott (Channing Laboratory, Brigham & Women's Hospital) for their assistance with the statistical analysis.

The study sponsors had no role in the design of the study; the collection, analysis, or interpretation of the data; the writing of the manuscript; or the decision to submit the manuscript for publication.

Manuscript received July 1, 2008; revised January 5, 2009; accepted January 28, 2009.